

Fracture Modeling of Crack Propagation in Wood and Wood Composites Including Crack Tip Processes and Fiber Bridging Mechanics

J. A. Nairn, N. Matsumoto

Wood Science & Engineering, Oregon State University, Corvallis, Oregon, USA

Abstract

Many materials develop process zones during fracture. For example, solid wood and wood composites develop process zones often consisting of fibers bridging the crack surfaces. After crack initiation, a process zone develops causing the toughness (or R curve) to increase with crack length. For materials with large process zones, the entire crack propagation data may be a rising R curve and thus there is a need to realistically model process zone development. This paper discusses the principles needed to model rising R curves, applies them in a new numerical model based on the material point method, and applies the concepts to crack growth in wood composites. Where previous models have used either fracture mechanics or cohesive zone methods, it will be argued that realistic modeling requires both fracture mechanics and a process zone.

1. Introduction

This paper is concerned with materials that develop process zones consisting of fibers bridging across the crack. Examples of such materials include solid wood [1], fibrous composites [2], wood composites [3], and cementitious composites [4]. Crack propagation experiments in such materials start with a machined notch; the crack tip of this initial notch has no process zone. As the load is applied a process or fiber-bridging zone develops. As a result, there are two crack tips — one at the actual crack tip at x_0 and one at the edge of the bridging zone defined here as the notch root at x_{root} (see Fig. 1). At early stages of crack propagation, the crack tip moves while the notch root remains stationary. The distance $x_{root} - x_0$ is the length of the developing bridging zone. Once the bridging zone is fully developed, the crack tip and notch root propagate together (barring the onset of edge effects) as steady-state or self-similar crack propagation.

In materials with bridging zones, one can measure the toughness as a function of crack growth known as the material's R curve. Typically the R curve starts at a minimum initial value and then rises as the bridging zone develops. Once self-similar crack propagation is reached, the R curve become constant at a steady-state toughness. If the bridging zone is short, the rising portion of the R curve will be short and the material can be characterized by its steady-state toughness. If the bridging zone is long, which in extreme cases may be longer than the specimen,

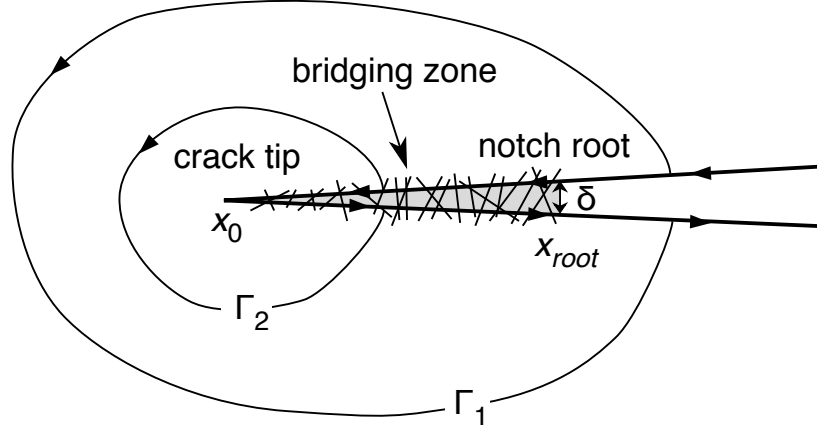


Fig 1: Crack tip region of a material with a fiber-bridging zone; x_0 is the location of crack tip and x_{root} is the location of the notch root. The contours Γ_1 and Γ_2 are for J integral evaluation inside and outside the fiber-bridging zone.

the rising portion of the R curve will be long; it may even encompass the entire experiment. For analysis of such materials, it is important to have good tools for analyzing bridging zone development. An accurate model can be used to extract material properties from the experimental results. This paper describes a model for rising R curves due to fiber bridging, an implementation of that model into numerical calculations using the material point method, and use of the numerical tool to analyze fiber bridging in the fracture of medium density fiberboard (MDF) and particle board (PB).

2. R Curve Analysis

The starting point for many prior analyses of fracture with a bridging zone is the far-field J integral, or a J integral for a contour outside the process zone (e.g., contour Γ_1 in Fig. 1). The far-field J integral for bridging zones with opening mode only can be shown to be [5]

$$J_{ff} = J_{tip} + \int_0^{\delta_{root}} \sigma(\delta) d\delta \quad (1)$$

where J_{tip} is energy release rate for crack tip propagation and the integral is the energy associated with crack tractions in the process zone; $\sigma(\delta)$ is the crack surface traction as a function of crack opening displacement, COD or δ (see Fig. 2), and δ_{root} is the COD at the notch root (at x_{root}). Physically, J_{ff} is the energy release rate associated with self-similar crack growth [6]. During self-similar crack growth, the bridging zone will be fully loaded, δ_{root} will equal the critical bridging law COD or δ_c , and the integral term in Eq. 1 will be the full area under the bridging law or J_B . The steady state toughness will be $J_{tip,c} + J_B$ where $J_{tip,c}$ is the toughness associated with crack tip processes.

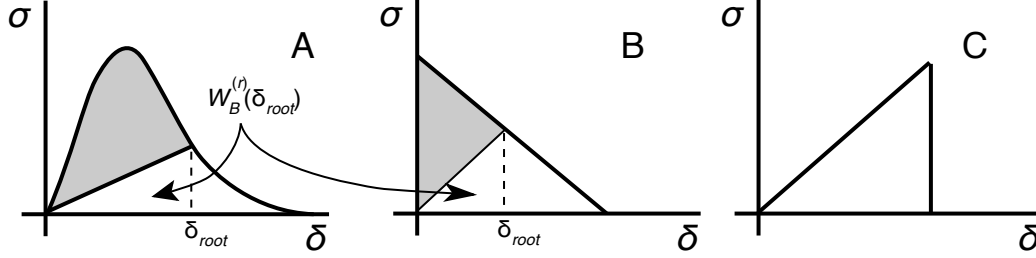


Fig. 2: Three sample fiber-bridging laws. The first two illustrate recoverable energy when the zone corresponds to an elastic process undergoing softening due to damage and the notch root has been loaded only to δ_{root} .

Crack propagation in the rising portion of the R curve, however, is non-self-similar because the process zone length is changing. Thus J_{ff} , in general, is not the correct energy release rate for that portion of the R curve. This fact has usually been ignored in prior work. In the rising portion, δ_{root} will be less than δ_c meaning both that the bridging zone will not be critical and the notch root will not be propagating. The actual energy released in this regime becomes [7]

$$R = J_{tip.c} + \int_0^{\delta_{root}} \sigma(\delta) d\delta - W_B^{(r)}(\delta_{root}) \quad (2)$$

where $W_B^{(r)}(\delta_{root})$ is the recoverable energy in the bridging zone when the notch root has been loaded to δ_{root} . Application of Eq. 2 to analysis of rising R curves requires insight into the mechanics of the bridging zone. Here it will be assumed that fiber bridging is an elastic process and that softening regimes in the bridging law are caused by fiber breakage or pull out. If the bridging zone is elastic, then unloading of the zone after damage will return linearly to the origin; the recoverable energy becomes the area under the unloading law (see Fig. 2A and 2B). By this assumption, the R curve becomes:

$$R = J_{tip.c} + \int_0^{\delta_{root}} \sigma(\delta) d\delta - \frac{1}{2} \sigma(\delta_{root}) \delta_{root} \quad (3)$$

Figure 3 shows sample R curves for cubic (Fig. 2A) and linear softening (Fig. 2B) bridging laws. The cubic law is sigmoidal in shape. The initial flat portion corresponds to the nearly linear elastic cubic bridging law at low δ . When the bridging law is linear elastic, most of the energy is recoverable and there is little increase in toughness. The linear softening law has no initial elastic region. Its R curve increases linearly until steady-state conditions at δ_c .

3. Numerical Modeling

The R curve concept of the previous section has been implemented into Material Point Method (MPM) modeling [7]. MPM worked well because of its ability to

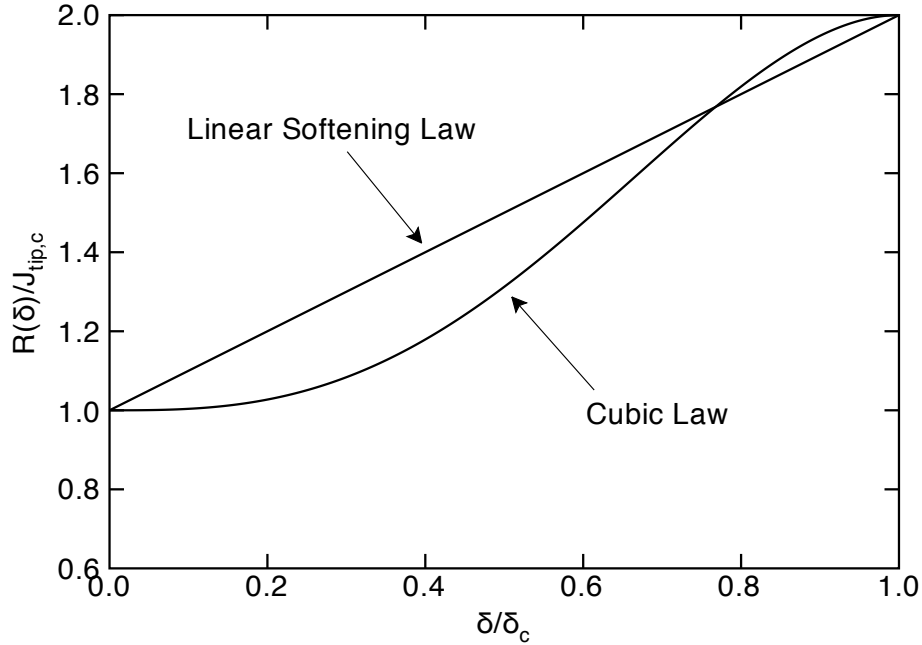


Fig. 3: Theoretical rising portions of R curves for an elastic fiber-bridging zone with a cubic bridging law or a linear softening bridging law. The bridging toughness was assumed to equal the crack tip toughness.

model explicit cracks with crack propagation in arbitrary directions [8] and to incorporate history-dependent traction laws on all or part of the crack surfaces [7]. Numerical fracture modeling with bridging zones proceeded as follows:

1. An explicit crack was introduced into the MPM model by defining a series of connected crack particles.
2. As the calculations proceed, J_{tip} was calculated. When $J_{tip} \geq J_{tip,c}$, the crack tip was allowed to propagate. For mode I cracks here, crack propagation was achieved by adding a new crack particle straight ahead of the crack tip. The new crack particle was assigned to the selected traction law with the COD initially equal to zero.
3. At the time of crack propagation, the actual energy released was calculated using Eq. 3.
4. For each time step, the COD on each crack particle was calculated and the notch root advanced whenever $\delta_{root} \geq \delta_c$.
5. The calculations continued until the crack length reached the end of the specimen.

This algorithm requires a numerical method that can calculate J_{tip} and an assumed bridging law, $\sigma(\delta)$. This capability was demonstrated for MPM in Ref. [7]. The required J_{tip} is

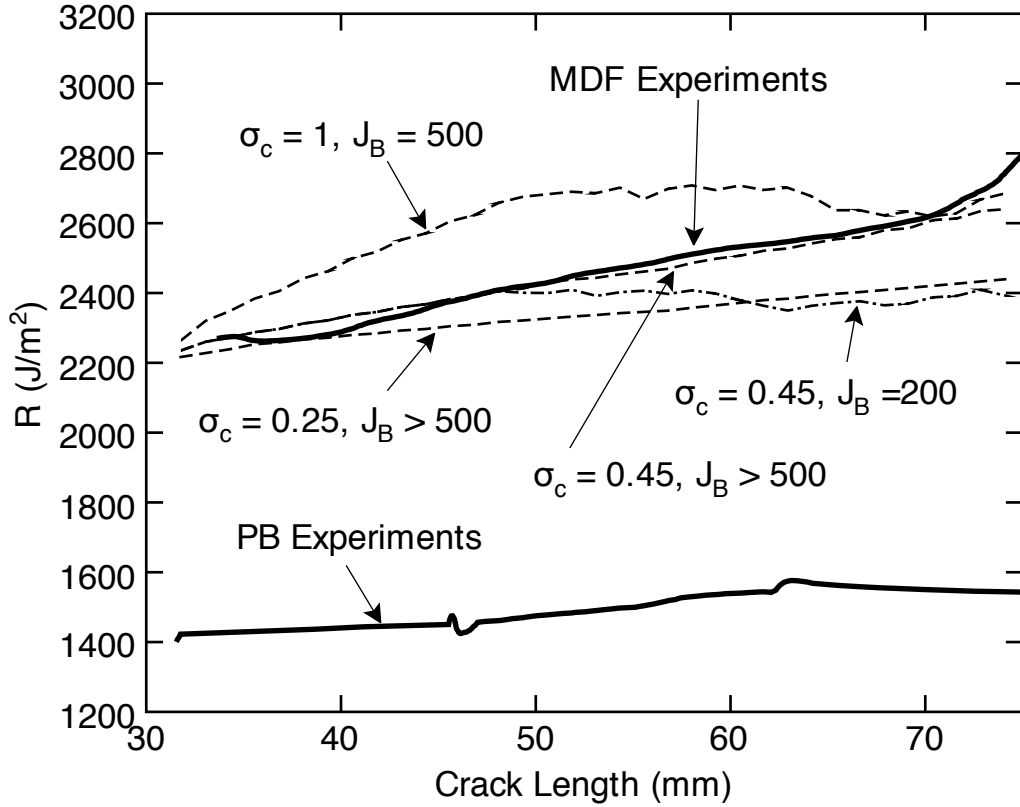


Fig. 4: Experimental R curves for MDF and PB (solid lines). The dashed and dash-dot lines are numerical simulation of MDF R curves for various values of cohesive stress, σ_c , and bridging toughness, J_B .

$$J_{tip} = \begin{cases} J(x) - \int_0^{\delta(x)} \sigma(\delta) d\delta & \text{if } x < x_{root} \\ J(x) - \int_0^{\delta_{root}} \sigma(\delta) d\delta & \text{if } x \geq x_{root} \end{cases} \quad (4)$$

where $J(x)$ is the usual J integral [6] using a contour from top to bottom crack surface starting and stopping at x , and $\delta(x)$ is the COD at the location of the contour. The top form is for contours inside the bridging zone such as Γ_2 in Fig. 1; the bottom form is for contours outside the bridging zone such as Γ_1 in Fig. 1. This evaluation of J_{tip} is independent of contour [7].

Examples of crack propagation simulations using the above algorithm are given in Ref. [7]. Notice that crack propagation can be accomplished by use of J_{tip} and bridging law alone. The only need for recoverable energy (the last term in Eq. 3) is in the step for calculating the energy released. This output of the calculation plays no role in the crack growth mechanics, but is essential for calculating R curves.

4. Analysis of MDF and Particle Board Experiments

We ran mode I crack propagation experiments on medium density fiberboard (MDF) [3]. MDF is a wood-based composite with fine wood fibers bound together by a small amount of adhesive [9]. Although crack propagation could not be detected optically, we were able to monitor crack growth using digital image correlation methods [3,10]. By combining crack growth measurements with direct measurements of energy released, we were able to determine an experimental R curve for MDF. One experimental result is shown as the solid line in Fig. 4 for MDF with a density of 609 kg/m^3 (38 lbs/ft^3). The initial toughness is about 2200 J/m^2 and it increases roughly linearly with crack length. The R curve never reaches steady-state crack propagation. The rapid rise after crack length of 70 mm is an edge effect [3].

The linear R curve suggests a linear softening law, as guided by the theoretical results for a linear softening law in Fig. 3. The experimental results, however, are for R as a function of crack length and not as a function of COD. Some numerical calculations with the compact tension geometry used in the experiments showed that notch root COD is roughly proportional to crack growth. Thus a linear response in crack length implies a linear response in notch root COD as well.

The experimental results are best interpreted by direct numerical simulation using the techniques in the previous section. Figure 4 compares simulations to experimental results for various values of cohesive stress, σ_c , and bridging toughness, J_B . The dashed lines are for $\sigma_c = 0.25, 0.45,$ and 1 MPa with $J_B = 500 \text{ J/m}^2$; all simulations used $J_{ip,c} = 2210 \text{ J/m}^2$. All simulated R curves are linear in crack length. Their slopes increased with σ_c . A value of $\sigma_c = 0.45 \text{ MPa}$ agreed with the experimental results. For $\sigma_c = 1 \text{ MPa}$, the simulations reached steady state at a crack length of about 50 mm . Like the experiments, the simulations for $\sigma_c = 0.25$ and 0.45 MPa did not reach steady state. The dashed-dot line is for $\sigma_c = 0.45 \text{ MPa}$ with $J_B = 200 \text{ J/m}^2$. Because of the lower J_B , this simulation reached steady state at a crack length of about 50 mm . The initial slope, however, was identical to the other $\sigma_c = 0.45 \text{ MPa}$ simulation, which confirms that the slope is a function only of σ_c .

Because the experiments never reached steady state, it was not possible to measure either J_B or δ_c . By using numerical simulations, however, the cohesive stress could uniquely be determined. It is also possible to place bounds on J_B and δ_c by assuming the experiments were on the verge of reaching steady state. By this analysis, we determined $J_B \geq 500 \text{ J/m}^2$ and $\delta_c \geq 2.57 \text{ mm}$ [3]. Interestingly, δ_c is close in magnitude to the expected wood fiber length in MDF made from softwood of $3\text{-}4 \text{ mm}$ [9].

Also shown in Fig. 4 are new experiments on particle board (PB) with a density of 708 kg/m^3 (44 lbs/ft^3). Like MDF, PB is a wood-based composite, but unlike MDF, PB is comprised of wood particles rather than wood fibers. The experimental R curve measured by the same methods shows little increase in toughness. The toughness of PB is thus about 1450 J/m^2 with little or no fiber bridging effects.

In the past, numerical fracture models have tended to use *either* fracture mechanics criteria *or* cohesive zones models (CZM) [11]. In the above experiments, the MDF experiments would be interpreted with a CZM model while the PB results would use a fracture mechanics model. The interpretations of the two materials would be vastly different. The MPM modeling here is a generalization of numerical fracture modeling to use *both* fracture mechanics *and* a fiber-bridging zone [7]. Fracture mechanics methods were used to model crack-tip processes. Traction-law methods were used to model the bridging zone. The interpretations for MDF and PB become more similar and more physical. MDF is slightly tougher in the crack tip region and the wood fibers contribute to an increase in toughness as the crack propagates. The extent of bridging is related to the wood fiber length. In contrast, PB is lower in toughness and the particles provide little or no toughness enhancement during crack propagation.

References

- [1] I. Smith, S. Vasic, Fracture behaviour of softwood, *Mechanics of Materials* 35 (8) (2003) 803–815
- [2] S. Hashemi, A.J. Kinloch, J.G. Williams JG, The analysis of interlaminar fracture in uniaxial fibre reinforced polymer composites, *Proc R Soc Lond A347* (1990) 173–199
- [3] N Matsumoto, J.A. Nairn, The fracture toughness of medium density fiberboard (MDF) including the effects of fiber bridging and crack-plane interference, *Engr. Fract. Mech.* submitted (2008).
- [4] V. C. Li, C.M. Chan, C.K.Y. Leung, Experimental determination of the tension-softening relations for cementitious composites, *Cement and Concrete Research* 17 (1987) 441–452
- [5] G. Bao, Z. Suo, Remarks on crack-bridging concepts, *Appl Mech Rev* 45 (6) (1992) 355–366
- [6] J.R. Rice, A path independent integral and the approximate analysis of strain concentration by notches and cracks, *J Applied Mech* June (1968) 379–386
- [7] J.A. Nairn. Analytical and Numerical Modeling of R Curves for Cracks with Bridging Zones, *Int. J. Fracture* in press (2008)
- [8] J.A. Nairn, Material point method calculations with explicit cracks, *Computer Modeling in Engineering & Sciences* 4 (2003) 649–664

- [9] J.J. Bower, R. Shmulsky, J.G. Haygreen, Forest Products and Wood Science - An Introduction, 4th Edition, Iowa State Press, Ames, IA, 2003.
- [10] S. Samarasinghe, G.D. Kulasiri, Displacement fields of wood in tension based on image processing: Part 1, *Silva Fennica* 34 (3) (2000). 251-259
- [11] B.R.K. Blackman, H. Hadavinia, A.J. Kinloch, J.G. Williams, The use of a cohesive zone model to study the fracture of fibre composites and adhesively bonded joints, *Int J Fract* 119 (2003) 25–46